

Density dependence of the forbidden lines in Ni-like tungsten

This article has been downloaded from IOPscience. Please scroll down to see the full text article.

2007 J. Phys. B: At. Mol. Opt. Phys. 40 F175

(<http://iopscience.iop.org/0953-4075/40/11/F01>)

View [the table of contents for this issue](#), or go to the [journal homepage](#) for more

Download details:

IP Address: 38.107.179.211

The article was downloaded on 21/02/2012 at 03:55

Please note that [terms and conditions apply](#).

FAST TRACK COMMUNICATION

Density dependence of the forbidden lines in Ni-like tungsten

Yuri Ralchenko

Atomic Physics Division, National Institute of Standards and Technology, Gaithersburg, MD 20899-8422, USA

E-mail: yuri.ralchenko@nist.gov

Received 2 April 2007, in final form 5 April 2007

Published 23 May 2007

Online at stacks.iop.org/JPhysB/40/F175

Abstract

The magnetic-octupole (M3) and electric-quadrupole (E2) transitions between the ground state $3d^{10} \ ^1S_0$ and the lowest excited $3d^94s \ (5/2, 1/2)J = 3$ and $J = 2$ states in the Ni-like tungsten are shown to exhibit a strong dependence on electron density N_e in the range of values typical for tokamak plasmas. Remarkably, the total intensity of these overlapping lines remains almost constant, which may explain the strong emission in the 7.93 Å line observed in tokamak experiments (Neu R *et al* 1997 *J. Phys. B: At. Mol. Opt. Phys.* **30** 5057). Utilization of the M3 and E2 line ratios for density diagnostics in high-spectral-resolution experiments is discussed as well.

(Some figures in this article are in colour only in the electronic version)

Since tungsten is considered to be a strong candidate for one of the plasma-facing components in the next-generation tokamaks, the x-ray spectra from its highly charged ions are being actively studied in fusion devices, e.g. ASDEX Upgrade tokamak [1, 2], and in electron beam ion traps (EBIT) [3, 4]. The measured spectra are used to infer diverse and substantial information on plasma parameters and to test advanced atomic structure theories and collisional-radiative models.

The forbidden radiative transitions from highly ionized tungsten are routinely observed in x-ray and extreme ultraviolet (EUV) spectral regions [5–7]. The Einstein coefficients for forbidden lines strongly depend on the ion spectroscopic charge Z_{sp} , so that for 40–50 times ionized tungsten atoms the electric-quadrupole (E2), magnetic-dipole (M1) and even magnetic-octupole (M3) transition probabilities are sufficiently strong to overcome collisional quenching in low-density plasmas. Since the intensities of the forbidden lines are sensitive to the balance of radiative and collisional processes, they often serve as an important diagnostic tool in fusion, astrophysical and laboratory plasmas (see, e.g., [8]).

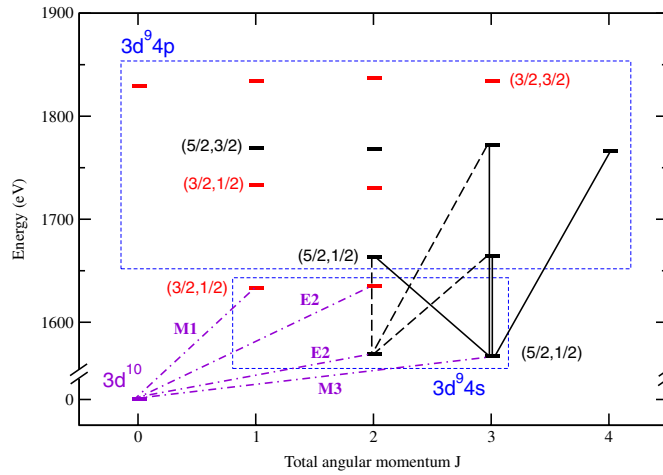


Figure 1. Energy scheme of the $3d^{10}$, $3d^9 4s$ and $3d^9 4p$ configurations in Ni-like tungsten. The forbidden $3d^{10}$ – $3d^9 4s$ transitions are shown by dot-dashed lines with transition types indicated next to lines. The excited levels with the total angular momentum of the $3d^9$ core $J_c = 5/2$ are shown in black and the $J_c = 3/2$ levels are shown in red. The dominating excitation channels from the $(5/2, 1/2)_3$ level are shown by solid lines, and the E1 radiative transitions into the $(5/2, 1/2)_2$ level are shown by dashed lines.

One of the most prominent lines observed in the x-ray spectra of highly charged tungsten is a spectral line at 7.93 \AA ,¹ which originates from the Ni-like ion W XLVII. (See, for instance, figure 3 of [2] and figure 1 of [3].) This line is, in fact, an overlap of two forbidden lines, namely, the M3 line $3d^{10} \text{ } ^1S_0$ – $3d^9 4s (5/2, 1/2)_3$ and the E2 line $3d^{10} \text{ } ^1S_0$ – $3d^9 4s (5/2, 1/2)_2$ with theoretical wavelengths of about 7.94 \AA and 7.93 \AA , respectively, as confirmed by several independent calculations [3, 9, 10]. In [3], we showed that in order to correctly calculate the intensity of the 7.93 \AA line in a low-density plasma of EBIT, one has to accurately take into account both M3 and E2 transitions. We also discussed the identification and population mechanisms for all four forbidden lines between the first excited configuration $3d^9 4s$ and the ground state $3d^{10} \text{ } ^1S_0$. These transitions (see table 1) are indicated by dot-dashed lines in figure 1, which presents the energy structure of the $3d^{10}$, $3d^9 4s$, and $3d^9 4p$ configurations in the Ni-like tungsten. For such a highly charged heavy ion, jj-coupling is the most appropriate coupling scheme, which is confirmed by the level grouping into jj-terms (figure 1).

For diagnostic purposes it is important to know whether the M3 line, with its small transition probability of $A_{M3} \approx 9 \times 10^3 \text{ s}^{-1}$, would be collisionally quenched in tokamak plasmas with electron density $N_e \sim 10^{14} \text{ cm}^{-3}$, which is about three orders of magnitude higher than that in an EBIT. To address this problem, we calculate here the intensities of the $3d^{10}$ – $3d^9 4s$ forbidden lines for a wide range of electron densities N_e from 10^{11} cm^{-3} to 10^{15} cm^{-3} and electron temperatures T_e from 1000 eV to 5000 eV . This span of densities and temperatures covers the typical values in tokamaks [1, 2]. The line intensities are calculated using the collisional-radiative code NOMAD [11] and the relativistic atomic structure and collision code FAC [12]. The details of our modelling are described elsewhere [3], the

¹ The wavelength determined from the tokamak spectra [1, 2] was 7.94 \AA , while our recent EBIT measurements [3] gave a slightly smaller value of 7.93 \AA . For consistency, it is the latter wavelength that is being used throughout this paper.

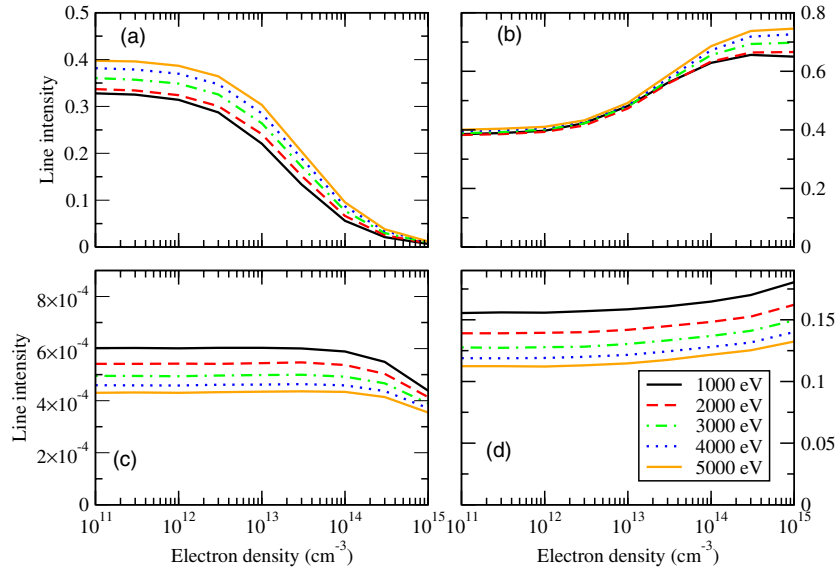


Figure 2. Calculated intensities (relative to the E1 $3d^{10} 1S_0-3d^9 4f (3/2, 5/2)_1$ line intensity) for the forbidden lines $3d^{10}-3d^9 4s$ as a function of electron density for $T_e = (1000-5000)$ eV: (a) M3 line $1S_0-(5/2, 1/2)_3$, (b) E2 line $1S_0-(5/2, 1/2)_2$, (c) M1 line $1S_0-(3/2, 1/2)_1$ and (d) E2 line $1S_0-(3/2, 1/2)_2$.

Table 1. Calculated wavelengths (in Å) and transition probabilities (in s^{-1}) for forbidden transitions $3d^{10} 1S_0-3d^9 4s$ in Ni-like tungsten. Notation a[b] denotes $a \times 10^b$.

Type	Upper level	Wavelengths (Å)			Transition probabilities (s^{-1})		
		Reference [3]	Reference [9]	Reference [10]	This work	Reference [9]	Reference [10]
M3	$(5/2, 1/2)_3$	7.940	7.945	7.938	9.35 [3]	–	8.22 [3]
E2	$(5/2, 1/2)_2$	7.930	7.935	7.929	5.94 [9]	5.92 [9]	5.32 [9]
M1	$(3/2, 1/2)_1$	7.616	7.620	7.614	1.37 [4]	–	1.63 [4]
E2	$(3/2, 1/2)_2$	7.610	7.614	7.608	4.55 [9]	4.51 [9]	4.04 [9]

only difference being the use of a Maxwellian electron energy distribution function for the thermal tokamak plasma discussed here. The simulations were performed in the steady-state approximation. Although here we included six ionization stages from W XLV to W L with total of more than 2400 levels, the main conclusions can be derived by considering only the levels within the Ni-like W XLVII.

It is convenient to present the results in terms of the line intensities relative to the strongest dipole-allowed (E1) line in the Ni-like ion, namely, the $3d^{10} 1S_0-3d^9 4f (3/2, 5/2)_1$ transition at 5.689 Å. These intensity ratios for the four $3d^{10}-3d^9 4s$ forbidden lines are shown in figure 2. At lowest densities, the relative intensity for the weak M3 line $1S_0-(5/2, 1/2)_3$ (figure 2(a)) is seen to remain approximately constant up to $N_e \approx 10^{12} \text{ cm}^{-3}$. For higher electron densities, it indeed begins to decrease rapidly due to the collisional quenching of the upper level. However, the relative intensity for the strong E2 line $1S_0-(5/2, 1/2)_2$ with transition probability of $A_{E2} \approx 6 \times 10^9 \text{ s}^{-1}$ increases with density beginning from the same value of 10^{12} cm^{-3} (see figure 2(b)). As these two lines closely overlap, it is their total intensity

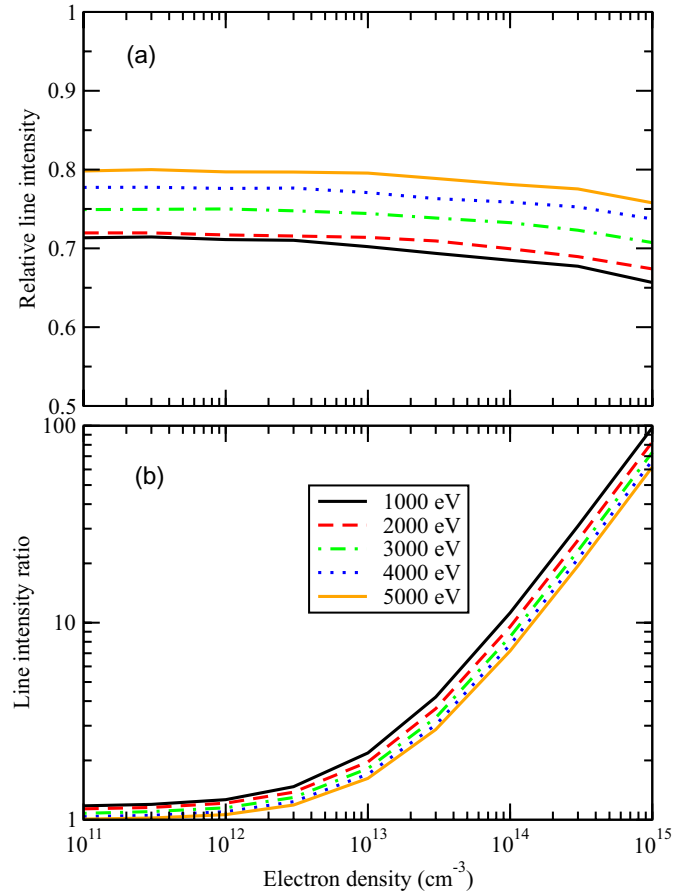


Figure 3. Calculated line intensities for $T_e = (1000\text{--}5000)$ eV: (a) sum of the relative intensities for the M3 line $^1S_0\text{--}(5/2, 1/2)_3$ and E2 line $^1S_0\text{--}(5/2, 1/2)_2$ and (b) ratio of line intensities I_{E2}/I_{M3} .

that has been measured in the tokamak and EBIT experiments. The total relative intensity, presented in figure 3(a), remains approximately *constant* over the whole range of densities from 10^{11} cm^{-3} to 10^{15} cm^{-3} . For instance, at the electron temperature of 4000 eV, which is close to experimentally measured values [1, 2], the intensity changes from about 0.78 at the lowest density to 0.76 at $3 \times 10^{13} \text{ cm}^{-3}$ and to 0.73 at 10^{15} cm^{-3} . This interplay between the M3 and E2 line intensities is certainly not accidental.

For low densities, the primary depopulation channel for the $3d^9 4s (5/2, 1/2)_3$ level is the M3 radiative decay: at $N_e = 10^{11} \text{ cm}^{-3}$ it is almost two orders of magnitude stronger than collisional depopulation. For higher densities, however, electron-impact collisions become more important so that at the typical tokamak value of $N_e = 3 \times 10^{13} \text{ cm}^{-3}$ the collisional excitation rate from the $3d^9 4s (5/2, 1/2)_3$ level is four times larger than the M3 transition probability. It is well known that the collisional excitation would preferentially go into the nearest levels that can be excited via dipole-allowed collisions, that is, the levels of the $3d^9 4p$ configuration (see figure 1). Moreover, the collisional rates are the strongest for those transitions that do not result in the rearrangement of the core $3d^9$. Therefore, in terms of *jj*-coupling, the excitation from the $3d^9 4s (5/2, 1/2)_3$ level with the total angular momentum

of the core $J_c = 5/2$ would primarily proceed into the $(5/2, 1/2)$ or $(5/2, 3/2)$ terms of the $3d^9 4p$ configuration.

It is also possible to determine which specific levels within those terms would be mainly populated via collisions. The selection rules for the dipole-allowed electron-impact excitation [13] indicate that for the s - p transitions, the final levels should have total angular momentum J_f differing by not more than one unit from the initial value J_i . Therefore, the excitation from the $3d^9 4s (5/2, 1/2)_3$ level would predominantly populate the $3d^9 4p$ levels with $J_f = 2, 3$ and 4. Indeed, our simulations show that at $N_e = 3 \times 10^{13} \text{ cm}^{-3}$ and $T_e = 4000 \text{ eV}$ this excitation channel amounts to more than 80% of the total collisional population outflux from this level.

The next important step in the determination of the population redistribution channels can be made by considering the radiative decays from the $3d^9 4p$ levels. Due to the $|\Delta J| \leq 1$ selection rule, the $J \geq 2$ levels of the $3d^9 4p$ configuration do not have allowed electric-dipole transitions into the ground state $3d^{10} {}^1S_0$. On the other hand, the $J_f = 2$ and 3 levels with $J_c = 5/2$ have strong ($A \approx 10^{10}$ – 10^{11} s^{-1}) E1 decays into the $3d^9 4s (5/2, 1/2)_2$ level, which is the upper level of the E2 line. (The $3d^9 4p (5/2, 3/2)_4$ level decays radiatively back into the $3d^9 4s (5/2, 1/2)_3$.) Since the electric-dipole radiative decays of the $3d^9 4p$ levels remain the dominant depopulation channel over a wide range of densities, at least up to $N_e \sim 10^{21} \text{ cm}^{-3}$, this in turn means that under tokamak conditions a significant part of the upward population flux from the $3d^9 4s (5/2, 1/2)_3$ level would be redirected into the $3d^9 4s (5/2, 1/2)_2$ level followed by the E2 transition into the ground state. Hence, although the collisional population redistribution between these two levels does modify the M3 and E2 line intensities, their sum intensity, i.e., the total intensity of the experimentally measured 7.93 Å line, remains almost constant over a large range of densities.

Although this unresolved 7.93 Å line seems to be insensitive to N_e , the intensity ratio of the M3 and E2 lines may become a very sensitive tool for density diagnostics in tokamak plasmas, provided these two lines can be resolved. Table 1 shows that the calculated wavelength difference $\Delta\lambda(\text{E2-M3})$ is about 0.010 Å, which is smaller than the experimental resolving limit of 0.015 Å of [1, 2]. The Doppler width in a plasma of $T_e = 4000 \text{ eV}$ is approximately 0.003 Å, so that a spectrometer with resolving power of several thousands would be sufficient to resolve the M3 and E2 lines. Figure 3(b) shows that the intensity ratio $I_{\text{E2}}/I_{\text{M3}}$ monotonically increases from ~ 1.7 at $N_e = 10^{13} \text{ cm}^{-3}$ to about 10 at 10^{14} cm^{-3} , and reaches almost 100 at 10^{15} cm^{-3} . This range of values makes the $I_{\text{E2}}/I_{\text{M3}}$ ratio well suited to density diagnostics in tokamaks.

One may ask whether other Ni-like ions might provide better opportunities for the determination of the density-dependent $I_{\text{E2}}/I_{\text{M3}}$ ratio. Since the $\Delta n = 0$ energy difference between the $(5/2, 1/2)_3$ and $(5/2, 1/2)_2$ levels of $3d^9 4s$ varies as Z_{sp} and the M3 and E2 transition energies are proportional to Z_{sp}^2 , the required resolution depends on the spectroscopic charge as $\lambda/\Delta\lambda \propto Z_{\text{sp}}^{-1}$. Although the fit of the results calculated with FAC in the range of $Z_{\text{sp}} = 29 - 58$ gives a slightly weaker dependence of $\lambda/\Delta\lambda \propto Z_{\text{sp}}^{-0.8}$, it would seem likely that using the elements heavier than tungsten would ease the spectral resolution requirements. However, this is not the case, primarily due to a very strong Z_{sp} -dependence, $A_{\text{M3}} \propto Z_{\text{sp}}^9$, for the M3 transition probability, which follows both from the present FAC calculations and from the results of [10]. It is obvious that the increasing A_{M3} combined with the $1/Z_{\text{sp}}$ dependence of the collisional $\Delta n = 0$ rates would shift the ratio sensitivity range towards higher densities, outside the typical tokamak values. Using elements lighter than tungsten, on the other hand, would drastically reduce the probability of the M3 decay and thus enhance the collisional quenching so that the M3 line would hardly be observed. It therefore seems quite peculiar that tungsten and close elements may be the most suitable for such diagnostic measurements.

Figures 2(c) and (d) also show the density dependence of the two other forbidden $3d^{10}-3d^94s$ lines, namely, the M1 line $^1S_0-(3/2, 1/2)_1$ and the E2 line $^1S_0-(3/2, 1/2)_2$. The M1 line at 7.616 Å (table 1) is seen to be extremely weak, which is due to a strong quenching M1 decay into the $(5/2, 1/2)_2$ level of the same configuration $3d^94s$ [3, 5], and therefore can hardly be observed. The second E2 line at 7.610 Å that has a high transition probability of $A \approx 4.5 \times 10^9 \text{ s}^{-1}$ exhibits a very weak dependence on N_e (figure 2(d)), increasing its relative intensity by only about 15% over the four orders of magnitude change in N_e . Thus, these two lines cannot be reliably used for density diagnostics in tokamak plasmas.

To summarize, we discussed here the density dependence of the intensities of the forbidden $3d^{10}-3d^94s$ lines in Ni-like tungsten. While the magnetic-octupole and electric-quadrupole lines from the lowest excited $(5/2, 1/2)$ term do show a strong dependence on N_e due to collisional redistribution of population between the levels, the total relative intensity of these overlapping lines does not change. This may explain the high intensity of the 7.93 Å line in the tokamak experiments. We also showed that, provided a high-spectral-resolution ($\lambda/\Delta\lambda \gtrsim 2000$) is achieved, the ratio of the E2 and M3 lines from the Ni-like tungsten can be used for density diagnostics in tokamaks.

Acknowledgments

This work was supported in part by the Office of Fusion Energy Sciences of the US Department of Energy. The author is grateful to J Reader and R Neu for valuable comments.

References

- [1] Neu R, Fournier K B, Schlögl D and Rice J 1997 *J. Phys. B: At. Mol. Opt. Phys.* **30** 5057
- [2] Neu R, Fournier K B, Bolshukhin D and Dux R 2001 *Phys. Scr.* T **92** 307
- [3] Ralchenko Yu, Tan J N, Gillaspay J D, Pomeroy J M and Silver E 2006 *Phys. Rev. A* **74** 042514
- [4] Neill P, Harris C, Safronova A S, Hamasha S, Hansen S, Safronova U I and Beiersdorfer P 2004 *Can. J. Phys.* **82** 931
- [5] Ralchenko Yu, Reader J, Pomeroy J M, Tan J N and Gillaspay J D 2007 in preparation
- [6] Pütterich T, Neu R, Beidermann C and Radtke R (ASDEX Upgrade Team) 2005 *J. Phys. B: At. Mol. Opt. Phys.* **38** 3071
- [7] Utter S B, Beiersdorfer P and Träbert E 2002 *Can. J. Phys.* **80** 1503
- [8] Griem H R 1997 *Principles of Plasma Spectroscopy* (Cambridge: Cambridge University Press)
- [9] Fournier K B 1998 *At. Data Nucl. Data Tables* **68** 1
- [10] Safronova U I, Safronova A S, Hamasha S M and Beiersdorfer P 2006 *At. Data Nucl. Data Tables* **92** 47
- [11] Ralchenko Yu V and Maron Y 2001 *J. Quant. Spectrosc. Radiat. Transfer* **71** 609
- [12] Gu M F 2004 *14th APS Topical Conference on Atomic Processes in Plasmas, AIP Proceedings* vol 730 (Melville, NY: AIP) p 127
- [13] Sobel'man I I, Vainshtein L A and Yukov E A 1995 *Excitation of Atoms and Broadening of Spectral Lines* (Berlin: Springer)